

Supplementary Information

Mapping ultrafast timing jitter in dispersion-managed 89 GHz frequency microcombs via self-heterodyne linear interferometry

Wenting Wang^{1,2,†}, Wenzheng Liu^{1,*,†}, Hao Liu^{1,†}, Tristan Melton¹, Alwaleed Aldhafeeri¹, Dong-IL Lee¹, Jinghui Yang¹, Abhinav Kumar Vinod¹, Jinkang Lim¹, Yoon-Soo Jang¹, Heng Zhou³, Mingbin Yu^{4,5}, Patrick Guo-Qiang Lo^{4,6}, Dim-Lee Kwong⁴, Peter DeVore⁷, Jason Chou⁷, Ninghua Zhu⁸ and Chee Wei Wong^{1,*}

¹ Fang Lu Mesoscopic Optics and Quantum Electronics Laboratory, University of California, Los Angeles, CA 90095, United States of America

² Mesoscopic Optics and Advanced Instruments Laboratory, School of Optics and Photonics, Beijing Institute of Technology, Beijing, China

³ Key Lab of Optical Fiber Sensing and Communication Networks, University of Electronic Science and Technology of China, Chengdu 611731, China

⁴ Institute of Microelectronics, A*STAR, Singapore 117865, Singapore

⁵ State Key Laboratory of Functional Materials for Informatics, Shanghai Institute of Microsystem and Information Technology, and Shanghai Industrial Technology Research Institute, Shanghai, China

⁶ Advanced Micro Foundry, Singapore 117685, Singapore

⁷ Lawrence Livermore National Laboratory, Livermore, CA 94550, United States of America

⁸ Institute of Intelligent Photonics, Nan Kai University, Tianjin, China

[†] These authors contributed equally to this work.

* To whom correspondence should be addressed. Email: wzliu@g.ucla.edu; cheewei.wong@ucla.edu

Supplementary Information Content

- I. Measurements of microcomb center frequency shift, timing jitter and pump intensity noise
- II. Characterizing the self-heterodyne linear interferometer frequency discrimination sensitivity and timing jitter measurement resolution
- III. Representative timing jitter performances of free-running passively mode-locked lasers.

I. Measurements of microcomb center frequency shift, timing jitter and pump intensity noise

The single-soliton microcomb center frequency shifts are measured in the dispersion-managed [62] and uniform microresonators, as shown in Figures S1a and S1b, respectively. In the dispersion-managed microresonator, the center frequency shift of the microcomb is negligible in

contrast with a 4.65 nm wavelength shift of a 2 μm waveguide width uniform microresonator when pumping at the similar wavelength.

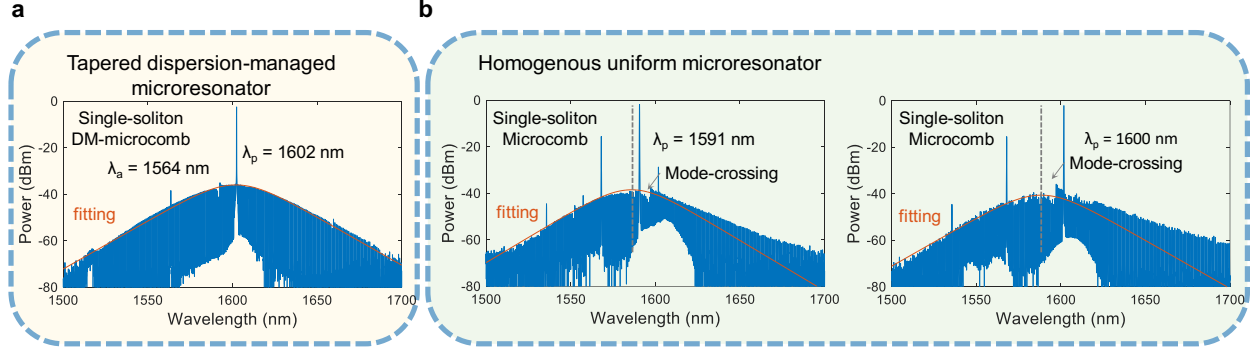


Figure S1 | Single-soliton optical spectra generated in the dispersion-managed and homogenous uniform microresonators. a, Single-soliton optical spectrum from a dispersion-managed microresonator. **b,** Single-soliton optical spectra generated in a uniform microresonator at different pump wavelengths.

A microresonator laser frequency comb in the mode-locked state is generated via the dual-driven pump approach, with a larger intracavity dispersion of $-150.8 \text{ fs}^2/\text{mm}$. We characterize the timing jitter with the self-heterodyne linear interferometer (SHLI), and subsequently compare with the original close-to-zero intracavity dispersion (path averaged GVD to $-4.39 \text{ fs}^2/\text{mm}$) mode-locked frequency microcomb. This is illustrated in Figure S2. Figure S2a and S2b show the measured cavity group velocity dispersion and the soliton microcomb optical spectrum. We observed that this larger dispersion microresonator increases the timing jitter to 14.37 fs integrated from 100 kHz to 10 kHz compared to our demonstration of the close-to-zero dispersion low-jitter state of $1.7 \pm 0.7 \text{ fs}$ as shown in Figure S2c. The Fourier frequency bandwidth of the measured timing jitter PSD is determined by our FFT analyzer bandwidth (SR 770 FFT Network Analyzer).

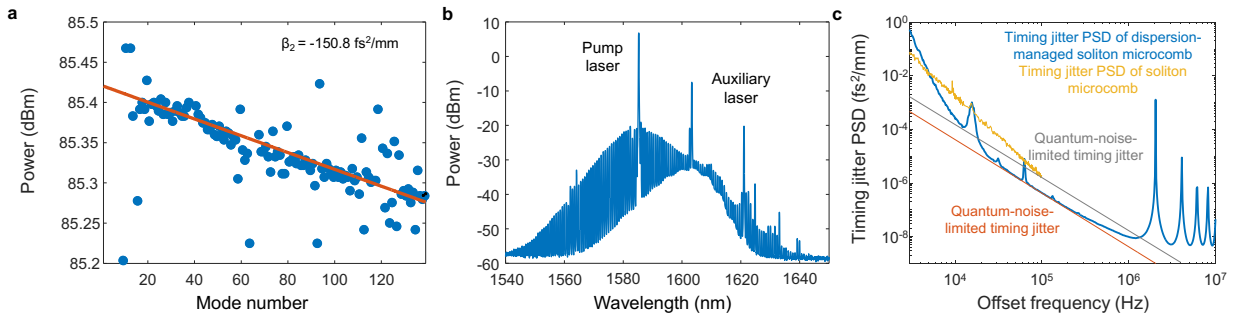


Figure S2 | Self-heterodyne linear interferometry measurement of timing jitter in the mode-locked soliton frequency microcomb, with larger intracavity dispersion in comparison with

close-to-zero dispersion microresonator. a, Measured cavity group velocity dispersion. **b,** Measured soliton microcomb optical spectrum. **c,** Measured timing jitter power spectral density.

Then, the pump laser intensity noise is characterized to illustrate the influence from electrical noise, EDFA noise, and free-space-to-chip coupling noise as shown in Figure S3. Measurements are conducted before the microresonator, after the microresonator when on and off resonance, and without the EDFA and are compared against the detector and instrumentation noise floor. From the RIN measurements, the free-space-to-chip coupling fluctuations below ≈ 7 kHz can be observed with additional intensity noise degradation. After the pump wavelength is tuned into the resonance, the extra coupling noise below 1 kHz is observed as well.

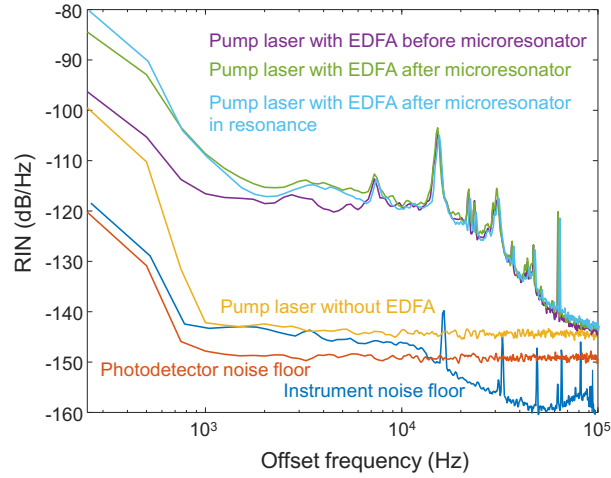


Figure S3 | The measured relative intensity noise (RIN) of the pump laser.

II. Characterizing the self-heterodyne linear interferometer frequency discrimination sensitivity and timing jitter measurement resolution

The fiber-delay-lined-based phase noise measurement is an averaged measurement [34,48,63,64]. The photodetected signal of each mode is filtered at f_{aom} and mixed by an RF mixer to reject the common-mode f_{ceo} noise. This downconverted RF mixer output contains the repetition-rate phase noise or timing jitter as a form of $\delta[\tau(m - n)f_{rep}]$. The frequency fluctuations of the two selected optical comb lines are converted into voltage fluctuations with the transfer function $\Delta V(f) \propto K_{\phi} \frac{|1 - e^{-i2\pi f\tau}|}{|i \times f|} (m - n) \Delta f_R(f)$ where K_{ϕ} is the peak voltage at the double-balanced mixer output. In our manuscript, we used 49-meter fiber for the timing jitter power spectral density measurement in the fiber Michelson interferometer which is noted in Figure 4 caption and Methods. The time delay is around 0.49 μ s corresponding to Fourier frequency of 2.04 MHz. This Fourier

frequency set the upper offset frequency bound for our measurement. For the self-heterodyne linear interferometry timing jitter measurement technique, the heterodyne beat note, frequency discrimination calibration and the measured frequency noise are illustrated in Figure S4. The heterodyne detection beat note magnitude and delay time determines the frequency discrimination sensitivity via: $\Delta V(f)/\Delta f_R(f) \propto K_\varphi \frac{|1 - e^{-i2\pi f\tau}|}{|i \times f|} (m - n)$.

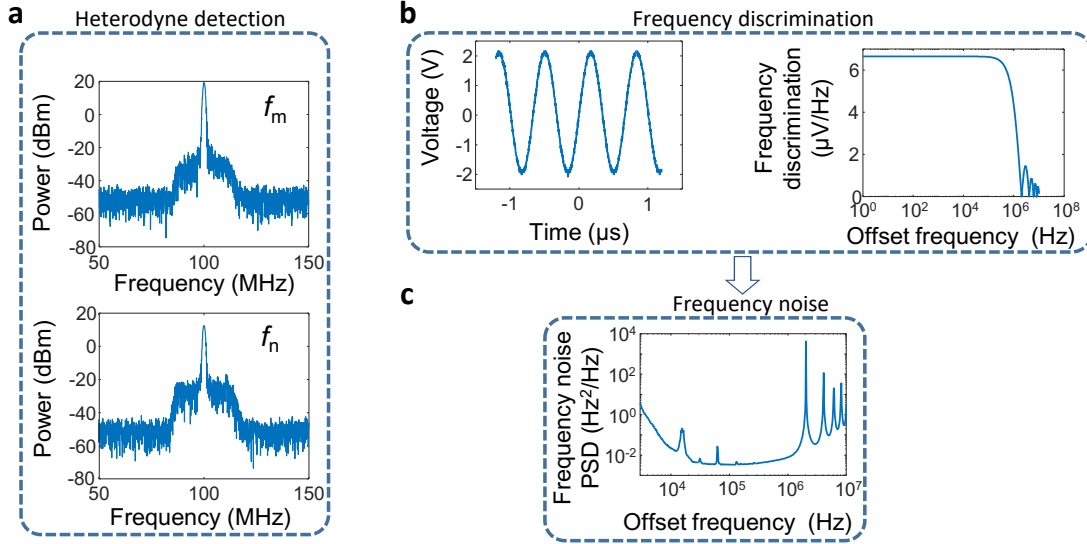


Figure S4 | Frequency discrimination and timing jitter measurement calibration. **a**, Example measured heterodyne beat note at the 100 MHz frequency. **b**, Frequency discrimination calibration of the system at 6.75 μ V/Hz from 1 to 100-kHz offset. **c**, Measured frequency noise power spectral density of 3- Hz^2/Hz at 3-kHz offset and 3×10^{-3} Hz^2/Hz at 100-kHz offset.

To characterize the system sensitivity, we carried out the experiment by setting $m = n$, wherein the noise floor is determined after common-mode noise rejection. The measured timing jitter measurement sensitivity is illustrated in Figure S5 where we set the delay time to $\tau = 489$ ns, 742 ns, and 1.24 μ s. First, we calibrate the timing jitter sensitivity as shown in Figure S5a which shows the timing jitter power spectral density noise floor of 1.6×10^{-10} fs^2/Hz . Over the same integrated frequency range of the timing jitter power spectral density, the integrated timing jitter is less than 0.1 fs. The system sensitivity calibration of sub-fs timing resolution shows the self-heterodyne linear interferometry could enable the femtosecond timing jitter characterization.

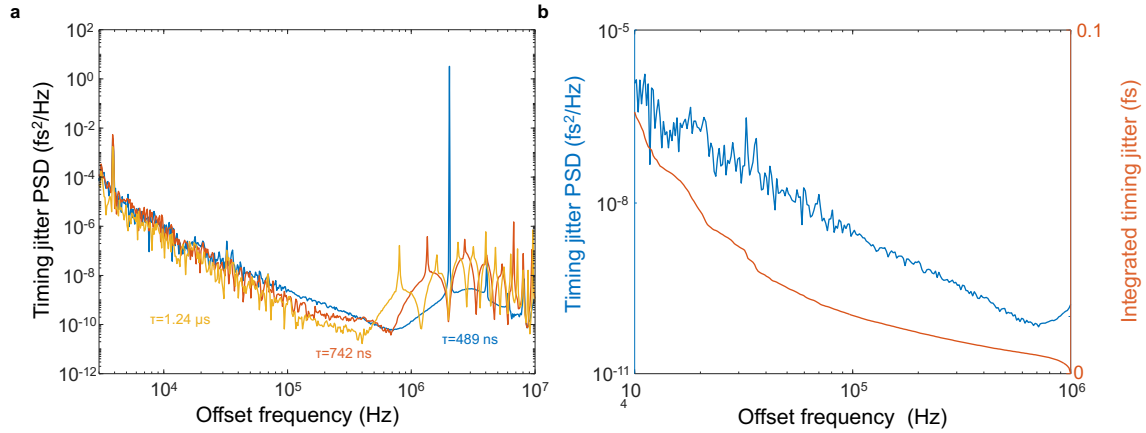


Figure S5 | The timing jitter measurement sensitivity. **a**, The determined timing jitter measurement sensitivity with different delay times. **b**, The determined timing jitter power spectral density and integrated timing jitter of the self-heterodyne linear interferometer noise floor.

III. Representative timing jitter and relative intensity noise performances of free-running mode-locked lasers.

Table S1 below summarizes the comparison of timing jitter in representative free-running mode-locked lasers. An example of applications enabled by the jitter-power tradeoffs can be seen in Ref. [68]. The chip-scale frequency microcombs provide a small size, weight, power and robustness compared to bulk mode-locked lasers. A low relative intensity noise is also helpful for applications in communications, and sensing. For example, a -153-dB/Hz would help in applications of optical communication for data processing. Most semiconductor diode lasers are in the range of -150 dB/Hz to -170 dB/Hz [69]. This is illustrated in Table S2 below.

Table S1 | Example jitter comparison of free-running mode-locked lasers.

Solid-state Laser /Fiber/ Microcavity	Timing jitter PSD at 10 kHz (fs^2/Hz)	Integrated timing jitter (fs)	Integrated Fourier frequency range	Measurement method
500 MHz, SESAM, Er:Yb-glass laser [65]	7×10^{-8}	0.016	[10 kHz - 250 MHz]	OH ^a
80 MHz, CNT-SA, soliton Er- fiber laser [66]	3×10^{-5}	0.5	[10 kHz - 40 MHz]	BOC ^a
80 MHz, NPR, soliton Yb-fiber laser [67]	6×10^{-4}	1.8	[10 kHz - 40 MHz]	BOC
20 GHz Silicon nitride frequency microcomb [12]	7×10^{-3}			High-speed detector
22 GHz silica microcombs [35]	1×10^{-3}	2.6	[10 kHz - 3 MHz]	FI ^c
22 GHz silica microcombs [44]	1×10^{-4}	—	—	BOC
89 GHz, dual-driven, soliton nitride microcomb [this work]	3×10^{-4}	1.7	[10 kHz - 1 MHz]	SHLI

BOC: Balanced optical cross-correlation; OH: optical heterodyne; FI: fiber interferometer; SHLI: self-heterodyne linear interferometer.

Table S2 | Example RIN comparison of free-running mode-locked lasers.

Example laser frequency comb system	Relative intensity noise [dB/Hz] at 1 kHz offset frequency	Relative intensity noise [dB/Hz] at 1 MHz offset frequency
500 MHz, SESAM, Er:Yb-glass laser [70]	-110	-140
1 GHz, SESAMa, soliton Yb:CALGO laser [71]	-115	-145
194 MHz, NPRa, soliton Er-fiber laser [72]	-140	-145
89 GHz, dual-driven, soliton nitride microcomb [this work]	-118	- 153